Effect of Bone Marrow-Derived Mesenchymal Stem Cells and Nanoscaffold on Wound Healing in Irradiated Rats



Ahmed Fouad,^A Marwa M. Hegab,^B Salwa Farid Ahmed,^A Soheir Korraa,^A Azza Ezz El-Arab^B

AHealth Radiation Research Department, National Center for Radiation Research and Technology (NCRRT), Atomic Energy Authority, Cairo, Egypt.

^BDepartment of Oral Medicine and Periodontology, Faculty of Oral and Dental Medicine, Cairo University, Cairo, Egypt.

Accepted for publication: January 30, 2023

Abstract

Background: The effect of bone marrow-derived mesenchymal stem cells (BM-MSCs) and nanoscaffolds were evaluated in enhancing wound healing in irradiated albino rats. Methods: Sixty-four male rats were subjected to 6 grays (Gy) of gamma (y)-rays. Surgical wounds were created on the rats' backs and they were randomly assigned to one of four groups (16 each); these were an irradiated control group, which did not receive treatment, an NS group treated with a nanoscaffold, a BM-MSC group injected subcutaneously with 1 million BM-MSCs, and a combination BM-MSC+NS group treated with BM-MSCs and a nanoscaffold. Wound healing was measured clinically and histologically. **Results:** The greatest reduction of anteroposterior wound dimensions was recorded in the BM-MSC+NS group (-69.79 ±19.27), followed by the NS group (-61.12 \pm 17.32), then the BM-MSC group (-43.89 \pm 20.04), and the least decrease was observed in the control group (-16.69 \pm 12.18) (p = 0.001). Meanwhile, the greatest reduction of lateral wound dimensions was recorded in the NS group (-60.41 ±11.80), followed by the BM-MSC+NS group (-45.23 ±62.82), then the BM-MSC group (-41.07 ±24.78), with the control group demonstrating the least reduction (-16.49 ± 20.90) (p = 0.008). Histologically, the combination group demonstrated the best healing results compared to the other groups. Conclusion: Nanoscaffolds and/or BM-MSC transplantation improved wound healing and regeneration in irradiated rats, providing possible therapeutic strategies for delayed wound healing during radiotherapy.

Keywords: Radiation; mesenchymal stem cells; nanoscaffold; healing

Introduction

Treatment of head and neck cancers with radiotherapy may subject patients to multiple oral complications, ranging from acute to chronic side effects. Radiation directly affects oral tissues including the vasculature, jaw muscles and bones, mucosal membranes, and salivary glands. Adverse reactions to radiotherapy depend on the volume and area being irradiated, total radiation dose and fractionation, patient's age and clinical condition, and associated treatments. Acute reactions which usually occur during treatment or weeks afterwards are often reversible, while chronic or late complications occurring

months or years after radiotherapy are irreversible.³

Compromised wound healing in irradiated tissues is a common and challenging clinical problem. Wound healing is a series of processes involving control of inflammation, cell migration, and new tissue remodeling.⁴ Radiation therapy causes changes in vascularity, regulatory growth factors, and fibroblasts, resulting in alteration in wound healing regardless of whether radiation was before or after surgery.⁵

Significant developments occurred in tissue engineering and stem cell-based therapies over the past decades.⁶ Mesenchymal stem cells (MSCs) are

undifferentiated cells that are able to selfrenew and possess a high proliferative capacity and mesodermal differentiation potential.⁷ Scaffolds also play a critical role tissue engineering and significant advances the development biodegradable polymers have been made. Electrospinning is a simple, low-cost method for producing nanofibers with a high surface area and a porous structure that has wide applications in tissue engineering, tissue repair substitutes, wound dressing materials, and carriers for drug delivery.8,9 Electrospun polymer nanofibers serve as skin substitutes as they can prevent fluid and protein loss from wound areas, help remove exudates, inhibit infection, exhibit antiadhesion properties, and guide endogenous cells to proliferate and remodel.¹⁰ Thus, our present study aimed to investigate the of bone marrow-derived mesenchymal stem cells (BM-MSCs) and nanoscaffolds in enhancing wound healing in irradiated albino rats.

Materials and Methods

Sample size was calculated using the G*Power software (version 3.1.9.7) to achieve a power of 1- β = 0.80 and a significance level of α = 0.05, resulting in 64 rats.¹¹ The simple randomization method was used by generating a random digit table.¹²

I. Animal Grouping and Surgical Procedure

Sixty-four male albino rats, weighing approximately 140-150 gm, were housed in the National Center for Radiation Research and Technology (NCRRT) of Egypt. The protocol was approved by Cairo University's Department of Animal Care, in accordance with the European Commission's guiding principles for care and use of laboratory animals, under approval number (CU III – S 62-17).

All rats received a single dose of 6 grays (Gy) of gamma (γ) radiation at a dose rate of 0.751 rad/s using a research

irradiator^a and were kept in quarantine for three days.¹³ Rats were randomly divided into four groups: an irradiated control group that did not receive treatment, an NS group treated with nanoscaffolds, a BM-MSC group injected subcutaneously with 1 million BM-MSCs and a combination BM-MSC+NS group treated with BM-MSCs and nanoscaffolds.¹⁴ Within each group, rats were further subdivided into two subgroups (eight each) according to the date of sacrifice.

II. Nanoscaffold Preparation

Nanoscaffold fibers were prepared using a nano fiber electrospinning unit at the NCRRT. Thirteen percent polycaprolactone (PCL) was dissolved in 1:1 chloroform: dimethylformamide, which was then sterilized using 25 kGy of cobalt-60 γ -radiation and examined through a scanning electron microscope (SEM).

Human MSCs were purchased from the Genetic Engineering Center at Al-Azhar University. The cells were categorized according to morphology, immunophenotyping (CD44+ and CD34-), and their ability to differentiate. They were counted using a hemocytometer, and surface markers were determined using a flow cytometer.^{c,5}

III. Wound Induction

On the third post-irradiation day, surgery was performed on 12-hour fasting rats under general anaesthesia. Ketamine^d 50 mg/kg body wight and xylazine (M.H. Reg. No. 1373/99 Vet; ADWIA, Egypt) 20 mg were injected intramuscularly in a 1:1 ratio, and 2% lidocaine^e was injected locally. The rats' backs were shaved and the site was prepared for surgery with consecutive applications of 10% povidone-iodine scrub and 70% isopropanol.

The surgical site was marked as a 1.5 cm diameter circle, a full-thickness wound was created, and tissues were discarded. The wound was washed with saline and either covered with a nanoscaffold (NS group), or

^a Gammacell® 40 Exactor, Best Theratronics Ltd. Ottawa, Ontario, Canada

^b JEOL Ltd., Japan

 $^{^{\}rm c}$ BD FACS Calibur $^{\rm TM}$ Flow Cytometer, BD Biosciences, Franklin Lakes, NJ, USA

d Ketam®, 50 mg/ml, EIPICO, Egypt

^e Alexandria Co. for Pharmaceuticals & Chemical Industries, Alexandria, Egypt

injected subcutaneously with 1 million BM-MSCs (BM-MSC group), or both (BM-MSC+NS group).¹⁴ The amount of injected material was uniformly distributed along the wound margins. Rats were placed in separate cages till the date of sacrifice.

IV. **Animal Sacrifice and Specimen Preparation**

Rats in each group were randomly subdivided into two subgroups (eight each) according to the date of sacrifice - either first or second week. Sacrifice performed with overdose anesthetic injections. 16 The wounded site was excised in a circular pattern, with normal tissue included in skin specimens, and then fixed in 10% buffered formalin and processed using a paraffin tissue processing machine. Tissue specimens were cut into 5 µ thick sections, mounted on glass slides, stained with hematoxylin and eosin (H&E) stain, and examined under a light microscope to evaluate histological changes during the healing process.

Other tissue sections were stained with Masson's trichrome stain to evaluate collagen fiber formation and orientation. The area percentage of collagen fibers was measured by the image analyzer computer system connected to the microscope via the Leica Qwin 500 software.f The image analyzer was first calibrated automatically to convert the measurement units (pixels) produced by the image analyzer programmer into actual micrometer units. The area percentage occupied by collagen fibers during wound healing was measured using an object lens of 20X magnification (total magnification of 200).

V. Clinical Evaluation and Area Measurement

Wounds were photographed using a Canon EOS 70D digital camerag and the area was measured using the Image J software.h,17 Wound surface area was quantified for all photographs using digitizing methods and the linear dimensions in the images were measured using the ruler tool in the Aperio ImageScopeⁱ viewing software. 18,19

Results

I. **Clinical Findings**

Anteroposterior and Lateral Wound Dimensions

At both weeks one and two, the highest mean values of anteroposterior and lateral wound dimensions were recorded in the control group, followed by the BM-MSC group, then the NS group, with the least value recorded in the BM-MSC+NS group. An analysis of variance (ANOVA) revealed a statistically significant difference between all groups (p = 0.00). At week one, Tukey's post hoc test revealed no significant difference between the NS group and the BM-MSC group, while at week two, there was no significant difference between the NS and the BM-MSC+NS groups. Moreover, the difference between anteroposterior wound dimensions of the NS group and the BM-MSC group was statistically insignificant (Table 1).

Within each group, the mean value of anteroposterior and lateral wound dimensions decreased significantly with time except for the lateral dimensions of the control group which demonstrated an insignificant reduction. The greatest difference anteroposterior of dimensions was recorded in the NS group, followed by the BM-MSC+NS group, then the BM-MSC group, and the least reduction was found in the control group. The Kruskal-Wallis test revealed a statistically significant difference between all groups (p = 0.027). The Mann-Whitney U test revealed that the difference between the NS, BM-MSC, and BM-MSC+NS groups was statistically nonsignificant, as was the difference between the control and BM-MSC. The greatest percentage reduction anteroposterior wound dimensions was recorded in the BM-MSC+NS followed by the NS group, then the BM-MSC group, with the least reduction being demonstrated in the control group. The difference between groups was statistically

f Leica Microsystems Inc., Wetzlar, Germany

g Canon Inc., Ōta, Tokyo, Japan

h National Institutes of Health, Bethesda, Maryland, USA

ⁱ Leica Biosystems, Wetzlar, Germany

significant according to the Kruskal-Wallis test (p = 0.00). The Mann Whitney U test revealed that the difference between the NS

group and the BM-MSC+NS group was statistically nonsignificant (Table 2).

Table 1. Descriptive statistics of anteroposterior and lateral wound dimensions and comparison between groups (ANOVA) and within each group (paired t-test)

Group		Mean ±SD	Mean ±SD	p -
		(mm)	(mm)	value
		1st Week	2 nd Week	
Anteroposterior Wound Dimensions	Control	1.35 ± 0.14^{a}	1.11 ± 0.10^{a}	0.01*
	NS	0.90 ±0.11 ^b	$0.35 \pm 0.16^{b,c}$	0.00*
	BM-MSC	1.01 ± 0.08^{b}	0.56 ± 0.19^{b}	0.00*
	BM-MSC+NS	0.69 ± 0.15^{c}	0.20 ± 0.12^{c}	0.00*
<i>p</i> -value		0.000*	0.000*	
Lateral Wound Dimensions	Control	1.54 ± 0.19^{a}	1.28 ± 0.32^{a}	0.06ns
	NS	0.90 ±0.16 ^b	0.36 ± 0.13^{c}	0.00*
	BM-MSC	1.03 ± 0.20^{b}	0.58 ± 0.21^{b}	0.01*
	BM-MSC+NS	0.59 ± 0.26^{c}	0.20 ± 0.12^{c}	0.01*
<i>p</i> -value		0.000*	0.000*	

Significance level: $p \le 0.05$; *significant; ns: nonsignificant; SD: standard deviation; Tukey's post hoc test: means sharing the same superscript letter are not significantly different.

Table 2. Difference between first and second week values and percentage change in values over time of anteroposterior and lateral wound dimensions (Kruskal-Wallis test)

	Group	Mean ±SD (mm)	Mean ±SD (%)
Anteroposterior Wound Dimensions	Control	-0.24 ±0.18 ^b	-16.69 ±12.18 ^c
	NS	-0.55 ± 0.17^{a}	-61.12 ± 17.32^{a}
	BM-MSC	$-0.45 \pm 0.23^{a,b}$	-43.89 ± 20.04^{b}
	BM-MSC+NS	-0.49 ± 0.19^{a}	-69.79 ±19.27 ^a
<i>p</i> -value		0.027*	0.00*
Lateral Wound Dimensions	Control	-0.26 ± 0.33	-16.49 ±20.90 b
	NS	-0.54 ± 0.11	-60.41 ±11.80 a
	BM-MSC	-0.45 ± 0.33	-41.07 ±24.78 a
	BM-MSC+NS	-0.39 ± 0.32	-45.23 ±62.82 a
<i>p</i> -value		0.28ns	0.008*

Significance level: $p \le 0.05$; *significant; ns: nonsignificant; SD: standard deviation; Mann Whitney U test: means sharing the same superscript letter are not significantly different.

The greatest difference in lateral wound dimensions was recorded in the NS group, followed by the BM-MSC group, then the BM-MSC+NS group, with the least reduction seen in the control group. The Kruskal-Wallis test showed a statistically nonsignificant difference between groups (p = 0.28). The greatest percentage reduction in lateral wound dimensions was recorded in the NS group, followed by the BM-MSC+NS group, then the BM-MSC group, with the least reduction seen in the control group. The Kruskal-Wallis test revealed that the difference between all groups statistically significant (p = 0.008), while the Mann-Whitney U test revealed that the difference between the NS, BM-MSC, and BM-MSC+NS groups was statistically nonsignificant (Table 2).

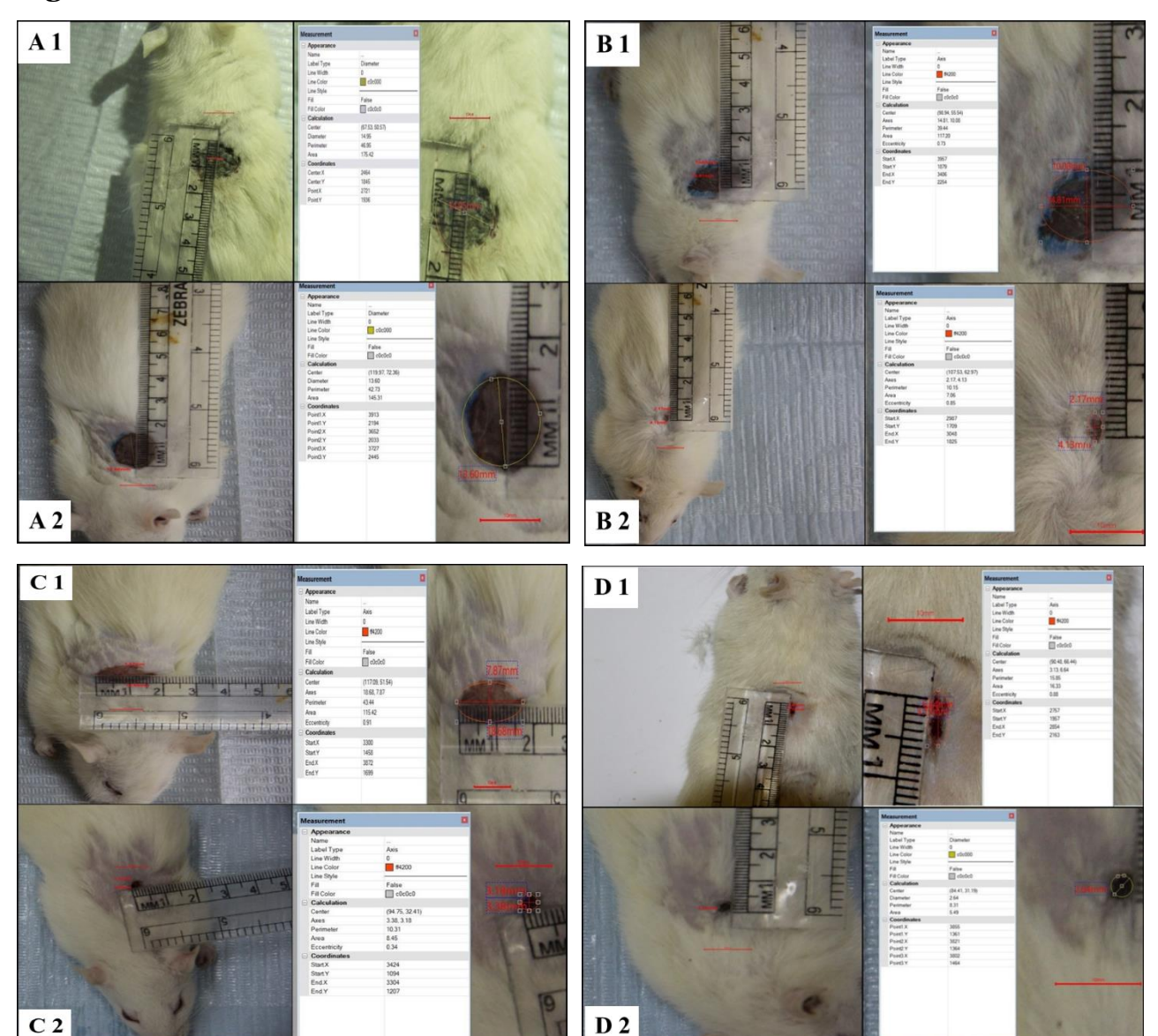
Area of Wound Recovery

Wound recovery was calculated by measuring the wound area at each time interval and comparing it with the original wound area (at the time of surgical procedure) as a percentage. One week postwounding, the least wound recovery was recorded in the control wound (1.69%), followed by the BM-MSC wound (34.21%), then the NS wound (38.15%), and the best

wound recovery was seen in the combination group BM-MSC+NS (88.55%). Two weeks post-wounding, the control wound showed the worst wound recovery (22.7%). The wounds of the BM-MSC and NS groups

expressed similar recovery percentages (95.22% and 95.7% respectively). The highest percentage of wound recovery was again detected in the BM-MSC+NS group (97.92%) (Figure 1).

Figure 1.



Measurements of wound dimensions for the control group (A1 and A2), for the NS group (B1 and B2), for the BM-MSC group (C1 and C2), and for the BM-MSC+NS group (D1 and D2) after the 1st and 2nd weeks respectively

II. **Histological Findings**

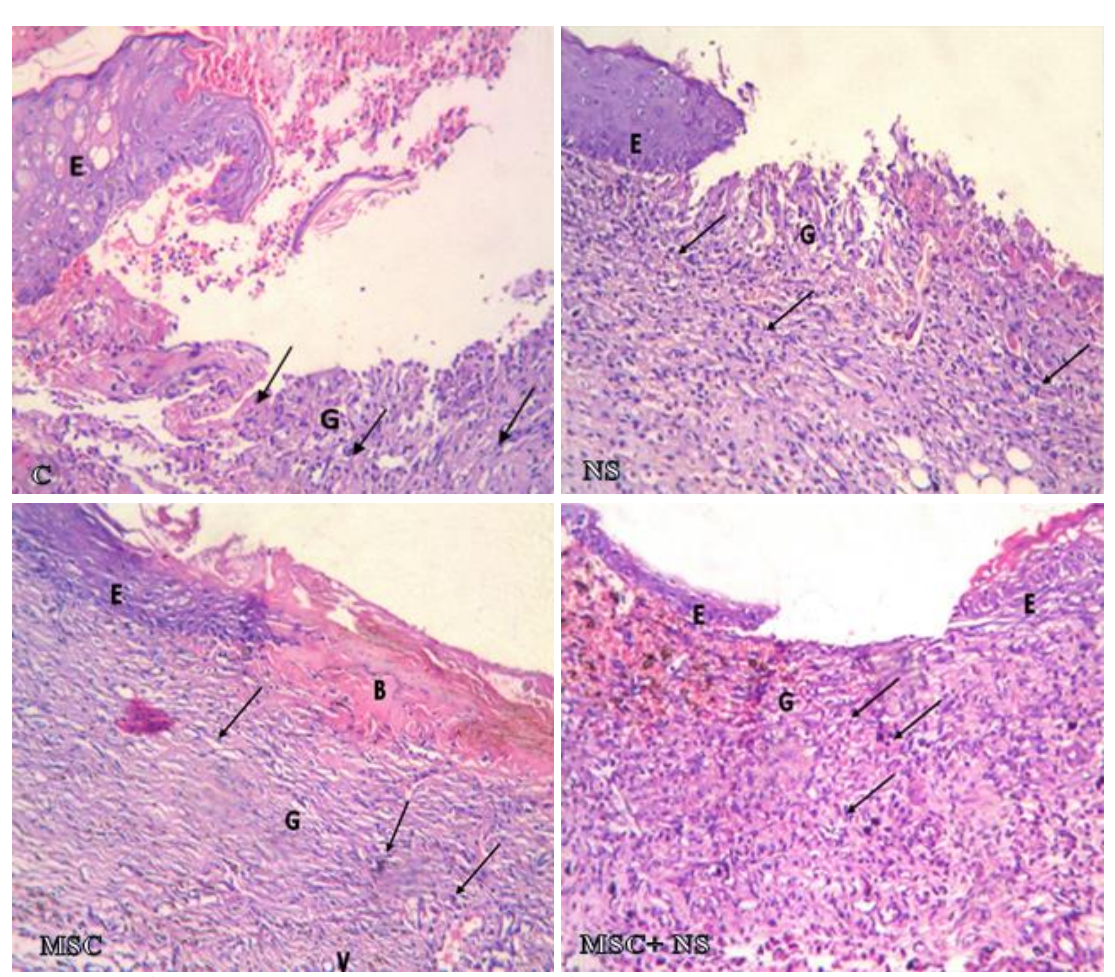
Hematoxylin and Eosin

One week post-wounding, the control group showed relatively large wounds with absence of granulation tissue. Chronic inflammatory infiltrate was detected in the wound bed and the margins of the epithelium showed vacuolization. The NS group demonstrated small wound sites, where the epithelium was normal at one edge and thin at the other. The wound gap was completely filled with granulation tissue infiltrated with chronic inflammatory cells. The BM-MSC group showed relatively large wound sites almost completely filled with granulation tissue with a mild chronic inflammatory cell

The BM-MSC+NS infiltrate. group demonstrated wounds that were fully covered with a blood clot and the underlying granulation tissue showed well-formed collagen fibers and a chronic inflammatory cell infiltrate (Figure 2).

Two weeks post-wounding, the edges of the control wound were approximated. However, the gap was deep, partially filled with granulation tissue, and not covered by epithelium. The granulation tissue was infiltrated with chronic inflammatory cells, and the gap was bordered with both acute and chronic inflammatory cells. The NS group demonstrated wound sites covered with intact, well-organized epithelium and the underlying dermis contained wellarranged collagen fibers, hair follicles, and sebaceous glands. The BM-MSC group had intact well-organized epithelium, with an underlying dermis showing more or less arranged collagen fibers, many hair follicles, and sebaceous glands. In the BM-MSC+NS group, the wound site was completely covered with normal epithelium, and the underlying dermis showed normal collagen fibers, sebaceous glands, and hair follicles many of which opened to the surface of the epithelium (Figure 3).

Figure 2.



Photomicrograph of dorsal skin at the wound site of irradiated control group (C) and treatment groups (NS, BM-MSC, and BM-MSC+NS) one week post-wounding; epithelium at the wound site (E), granulation tissue (G), chronic inflammatory cells (black arrows), blood clot (B), and blood vessels (V) are shown. [H&E x100]

Area *Percentage* Collagen Fiber **Formation**

At weeks one and two, the highest mean value with regards to the area percentage of collagen fiber formation was recorded in the BM-MSC+NS group, while the lowest value was recorded in the control group. An ANOVA revealed a statistically significant difference between all groups (p = 0.00). At week one, Tukey's post hoc test revealed no significant difference between the NS and the BM-MSC groups, while at week two, there was a significant difference between all groups. The mean value of area percentage of collagen fibers increased with time in all groups. The increase was significant in the NS group (p = 0.04), but nonsignificant in the control (p = 0.42), BM-MSC (p = 0.35),

and BM-MSC+NS (p = 0.24) groups (Table

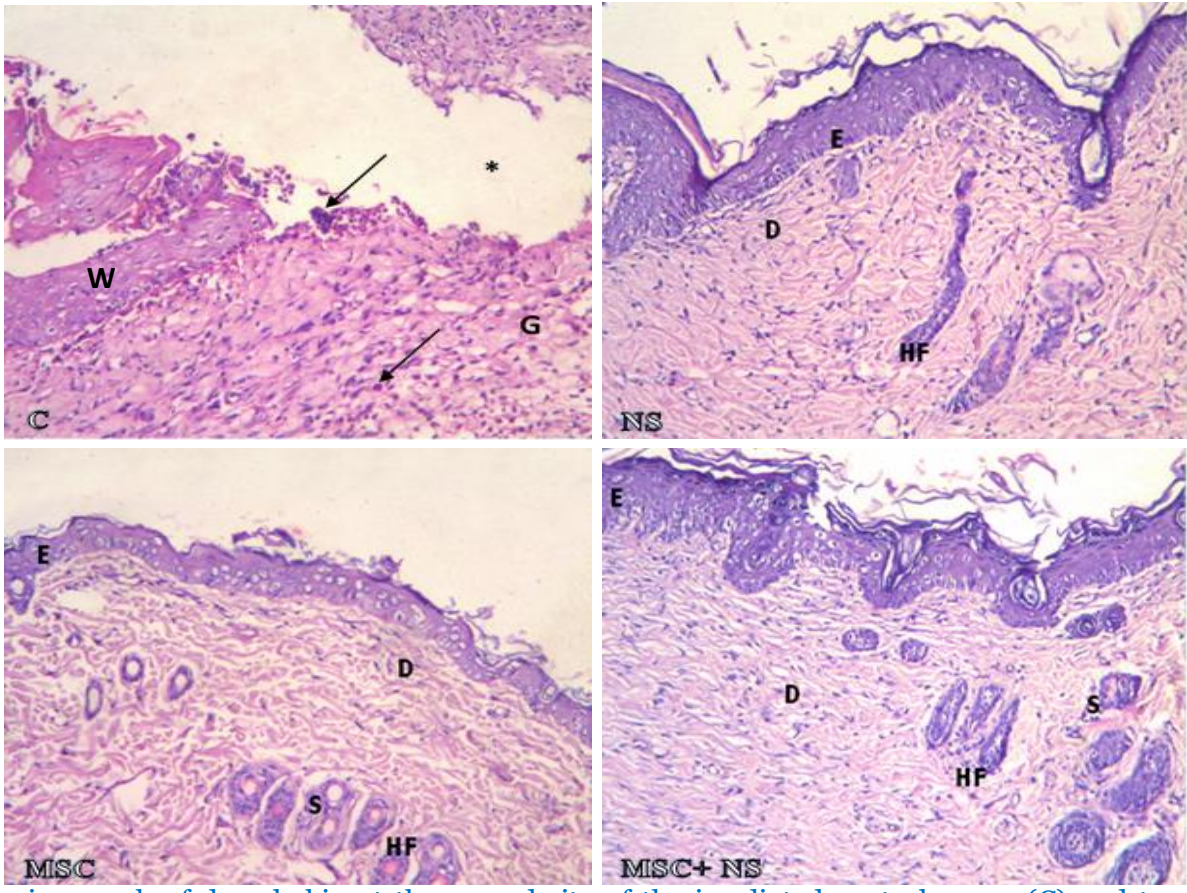
Discussion

Radiation contributes significantly delayed wound healing.20 cutaneous Normally, wound closure occurs within 14 days without radiation, while postirradiation wound closure might extend for over 30 days.21,22 Our study explored different treatment strategies for irradiated tissues and no obvious signs of infection, such as redness or swelling, were found in any treatment groups throughout the experiment. Only some scarring was noticed in the control and BM-MSC groups.

In our study, combing both BM-MSCs and nanoscaffolds showed the best results, and wounds treated with only nanoscaffolds provided better healing properties compared to those treated with BM-MSCs and compared to untreated irradiated rats. These findings are in accordance with Marquardt and Heilshorn who reported superior wound healing results in irradiated rats with wounds that were injected with MSCs throughout the edges and covered with a scaffold.²³ This is also in line with Chen et al. and Sun et al. who stated that electrospun scaffolds produce nano-fibrous meshes

comparable to the native extracellular matrix in a simple and versatile fashion.24,25 Nanofiber scaffolds support dimensional growth and infiltration of cells, which is essential in bioactive wound healing where a permissive scaffold is crucial for fibroblast and keratinocyte ingrowth and migration into wounds, and offer acellular skin substitutes that improve healing.^{26,27}

Figure 3.



Photomicrograph of dorsal skin at the wound site of the irradiated control group (C) and treatment groups (NS, BM-MSC, and BM-MSC+NS) two weeks post-wounding; epithelium at one side of the wound (W), granulation tissue at the base of wound bed (G), a gap in the center (*) still not covered by epithelium, chronic inflammatory cells (black arrows), intact epidermis with thin keratin layer at the wound site (E), normal underlying dermis (D), hair follicle (HF), and sebaceous gland (S) are shown. [H&E x100]

Table 3. Descriptive statistics and comparison of area percent in different groups (ANOVA test) and within each group (paired t-test)

Group	Mean ±SD (%)	Mean ±SD (%)	<i>p</i> -value
	1st Week	2 nd Week	
Control	19.08 ±6.01 ^c	22.07 ± 3.29^{d}	0.42ns
NS	40.96 ±6.77 ^b	50.89 ± 5.13^{b}	0.04*
BM-MSC	34.32 ± 8.30^{b}	41.19 ± 7.09^{c}	0.35ns
BM-MSC+NS	53.63 ± 7.25^{a}	61.90 ±6.67 ^a	0.24ns
<i>p</i> -value	0.000*	0.000*	

Significance level: $p \le 0.05$; *significant; ns: non-significant; SD: standard deviation; Tukey's post hoc test: means sharing the same superscript letter are not significantly different.

The absence of scarring in both nanoscaffold groups can be attributed to electrospinning, which provides a high surface area to volume ratio and has been

proven to promote cell-matrix interactions at the nanoscale.28,29 Nanoscaffolds also facilitate oxygen permeability and allow fluid accumulation, which highly prompts wound healing. Moreover, pores in nonwoven electrospun scaffolds (1-10 μm) are too small to allow bacterial penetration, resulting in resistance to infection and healing without scarring.30,31

The true mechanism of action of MSCs in accelerating wound closure has not yet been fully understood. However, it has been suggested that MSCs enhance wound repair through recruitment of inflammatory and progenitor cells, differentiation, and paracrine signaling.32 Ionizing radiation causes rapid and acute bone marrow suppression that is reversible in non-lethal doses. The tenable explanation of the superior wound healing found in the BM-MSC group compared to the control group could be due to their ability - when delivered to wounds externally - to provide a replacement and compensation for the progenitor cells suppressed in the bone after radiation marrow exposure.33 Mesenchymal stem cells possess significant potential for tissue damage therapy. They regulate can inflammation, apoptosis, promote angiogenesis, support the growth and differentiation of local stem and progenitor cells.34 Additionally, MSCs recruit fibroblasts and stimulate their migration from the surrounding tissues via chemotaxis.35,36

The reason why the BM-MSCs group ranked third after the combination and NS groups might be that the direct injection of BM-MSCs does not guarantee engraftment of transplanted cells and a lot of cells might have died upon injection.²³ It has been shown that the application of biomaterial carriers can protect the cells in the wound environment and support their viability and function.37

Histologically, our results support those of Levengood et al. who stated that at two weeks, a scab covered the width of the wound bed in the control group.38 **Hypertrophic** epidermis was present between the scab and the neo-dermal tissue re-epithelialization remained incomplete, whereas more collagen was present in the neo-dermis. A more mature, stratified neo-epidermis was present in the chitosan-PCL NS group, which was thicker than the normal epidermis surrounding the wound. Additionally, collagen deposition in the neo-dermis became more uniform in density.38 In Ma et al.'s study, necrotic

fibrinoid debris, inflammatory infiltration, capillary fibroblast and hyperproliferation was found in the control group on day 10, indicating that inflammation remained, while wounds in the NS group epithelialization demonstrated capillary hyperplasia. More layers keratinocytes were seen in the NS group, proliferating indicating the stage keratinocytes. A thin epidermal layer with several skin appendages were found in the NS group. The nanoscaffold group also demonstrated a higher amount of collagen production than the negative control. Transplanted accelerated **MSCs** formation of hair follicles and sebaceous probably glands most because promoted epithelial ingrowth chemotactic interaction and facilitated sending follicle progenitor cells toward the the wound center of during epithelialization.39

The present study revealed that tissue engineering combining electrospun nanoscaffolds and human **BM-MSC** transplantation improves wound healing regeneration in irradiated providing a possible therapeutic strategy for delayed wound healing during radiotherapy. Polycaprolactone nanoscaffolds suitable wound dressing that protects incisions from surgical the external environment and thus, preventing scar formation. The potential side effects of interspecies transplantation of MSCs have to be considered in future studies.

References

- 1. Peterson DE. Oral problems in supportive care: no longer an orphan topic? Support Care Cancer. 2000 Sep; 8(5):347-8. https://doi.org/10.1007/s0052000500
- 2. Chambers MS, Garden AS, Kies MS, JW. Radiation-induced Martin xerostomia in patients with head and neck cancer: pathogenesis, impact on quality of life, and management. Head Neck. 2004 Sep; 26(9):796-807. https://doi.org/10.1002/hed.20045
- 3. Specht L. Oral complications in the head and neck radiation patient. Introduction

- and scope of the problem. Support Care Cancer. 2002 Jan; 10(1):36-9. https://doi.org/10.1007/s00520010028
- 4. Lin TK, Zhong L, Santiago JL. Anti-Inflammatory and Skin Barrier Repair Effects of Topical Application of Some Plant Oils. Int J Mol Sci. 2017 Dec 27; 19(1):70. https://doi.org/10.3390/ijms19010070
- 5. Tibbs MK. Wound healing following radiation therapy: a review. Radiother 42(2):99-106. Oncol. 1997 Feb; https://doi.org/10.1016/s0167-8140(96)01880-4
- 6. Polak JM, Bishop AE. Stem cells and tissue engineering: past, present, and future. Ann N Y Acad Sci. 2006 Apr; 1068:352-66. https://doi.org/10.1196/annals.1346.00
- 7. Pittenger MF, Mackay AM, Beck SC, et al. Multilineage potential of adult human mesenchymal stem cells. Science. 1999 284(5411):143-7. 2; https://doi.org/10.1126/science.284.541 1.143
- 8. Meléndez-Ortiz H, Varca G, Lugão A, Bucio E. Smart Polymers and Coatings Obtained by Ionizing Radiation: **Synthesis** Biomedical and Applications. Open J Polym Chem. 2015 Aug; 5(3):17-33. https://doi.org/10.4236/ojpchem.2015. 53003
- 9. Jayakumar R, Menon D, Manzoor K, Nair SV, Tamura H. Biomedical Applications of Chitin and Chitosan based nanomaterials - A short review. Carbohydr Polym. 2010 Sep; 82(2):227https://doi.org/10.1016/j.carbpol.2010. 04.074
- 10. Sundaramurthi D, Krishnan UM, Sethuraman S. Electrospun Nanofibers as Scaffolds for Skin Tissue Engineering. Polym Rev. 2014 Apr; 54(2):348-76. https://doi.org/10.1080/15583724.2014 .881374

- 11. Faul F, Erdfelder E, Lang AG, Buchner A. G*Power 3: a flexible statistical power program for the analysis social, behavioral, and biomedical sciences. Methods. Behav Res2007 May; 39(2):175-91. https://doi.org/10.3758/bf03193146
- 12. Pocock SJ, Simon R. Sequential Treatment Assignment with Balancing for Prognostic Factors in the Controlled Clinical Trial. Biometrics. 1975 Mar; 31(1):103-15. https://doi.org/10.2307/2529712
- 13. Mehanni SS, Ibrahim NF, Hassan AR, Rashed LA. New approach of bone marrow-derived mesenchymal stem cells and human amniotic epithelial cells applications in accelerating wound healing of irradiated albino rats. Int J Stem Cells. 2013 May; 6(1):45-54. https://doi.org/10.15283/ijsc.2013.6.1.4 5
- 14. Abd-Allah SH, El-Shal AS, Shalaby SM, Abd-Elbary E, Mazen NF, Abdel Kader The role of placenta-derived mesenchymal stem cells in healing of induced full-thickness skin wound in a mouse model. IUBMB Life. 2015 Sep; 67(9):701-9. https://doi.org/10.1002/iub.1427
- 15. Lee TC, Lee TH, Huang YH, et al. Comparison of surface markers between human and rabbit mesenchymal stem cells. PLoSOne. 2014 9(11):e111390. https://doi.org/10.1371/journal.pone.01 11390
- 16. Monteiro BS, Faria RD, Coelho Zanella AR, et al. Mesenchymal stem cell infusion on skin wound healing of dexamethasone immunosuppressed wistar rats. Cienc Rural. 2016 Oct; 46(10):1824-9. https://doi.org/10.1590/0103-8478cr20151001
- 17. Chang AC, Dearman B, Greenwood JE. A comparison of wound area measurement techniques: visitrak versus photography. Eplasty. 2011 Apr 18; 11:e18.

- 18. Jørgensen LB, Sørensen JA, Jemec GB, Yderstraede KB. Methods to assess area and volume of wounds - a systematic review. Int Wound J. 2016 Aug; 13(4):540-53. https://doi.org/10.1111/iwj.12472
- 19. Hipp J, Cheng J, Daignault S, et al. Automated area calculation histopathologic features using SIVQ. CellPathol Anal (Amst).2011; 34(5):265-75. https://doi.org/10.3233/ACP-2011-
- 20. Spałek M. Chronic radiation-induced dermatitis: challenges and solutions. Clin Cosmet Investig Dermatol. 2016 Dec 9; 9:473-482. https://doi.org/10.2147/CCID.S94320
- 21. Tredget EE, Nedelec B, Scott PG, Ghahary A. Hypertrophic scars, keloids, and contractures. The cellular and molecular basis for therapy. Surg Clin North Am. 1997 Jun; 77(3):701-30. https://doi.org/10.1016/s0039-6109(05)70576-4
- 22. O'Sullivan B, Davis AM, Turcotte R, et al. Preoperative postoperative versus radiotherapy in soft-tissue sarcoma of the limbs: a randomised trial. Lancet. Jun 29; 359(9325):2235-41. https://doi.org/10.1016/S0140-6736(02)09292-9
- 23. Marquardt LM, Heilshorn SC. Design of Injectable Materials to Improve Stem Cell Transplantation. Curr Stem Cell Rep. 2016 Sep; 2(3):207-220. https://doi.org/10.1007/s40778-016-0058-0
- 24. Chen H, Fan X, Xia J, et al. Electrospun chitosan-graft-poly (εcaprolactone)/poly (ε-caprolactone) nanofibrous scaffolds for retinal tissue engineering. Int J Nanomedicine. 2011; 6:453-61. https://doi.org/10.2147/IJN.S17057
- 25. Sun B, Long Y, Zhang H, et al. Advances three-dimensional nanofibrous macrostructures via electrospinning. Prog Polym Sci. 2014 May; 39(5):862-90.

- https://doi.org/10.1016/j.progpolymsci. 2013.06.002
- 26. Singer AJ, Clark RA. Cutaneous wound healing. N Engl J Med. 1999 Sep 2; 341(10):738-46. https://doi.org/10.1056/NEJM1999090 23411006
- 27. Auger FA, Lacroix D, Germain L. Skin substitutes and wound healing. Skin Pharmacol Physiol. 2009; 22(2):94-102. https://doi.org/10.1159/000178868. Epub 2009 Feb 4. Erratum in: Skin Pharmacol Physiol. 2012; 25(2):110.
- 28. Zhang R, Ma PX. Synthetic nano-fibrillar extracellular matrices with predesigned macroporous architectures. J Biomed Mater Res. 2000 Nov; 52(2):430-8. https://doi.org/10.1002/1097-4636(200011)52:2<430::aidjbm25>3.0.co;2-l
- 29. Tan W, Krishnaraj R, Desai TA. Evaluation of nanostructured composite collagen--chitosan matrices for tissue engineering. Tissue Eng. 2001 Apr; 7(2):203-10. https://doi.org/10.1089/107632701300 062831
- 30. Huang ZM, Zhang YZ, Kotaki M, Ramakrishna S. A review on polymer nanofibers by electrospinning and their applications in nanocomposites. Compos Sci Technol. 2003 Nov; 63(15):2223-53. https://doi.org/10.1016/S0266-3538(03)00178-7
- 31. Khil MS, Cha DI, Kim HY, Kim IS, Bhattarai N. Electrospun nanofibrous polyurethane membrane as wound dressing. J Biomed Mater Res B Appl Biomater. 2003 Nov 15; 67(2):675-9. https://doi.org/10.1002/jbm.b.10058
- 32. Chen L, Tredget EE, Wu PY, Wu Y. Paracrine factors of mesenchymal stem cells macrophages recruit and endothelial lineage cells and enhance wound healing. PLoS One. 2008 Apr 2; 3(4):e1886. https://doi.org/10.1371/journal.pone.oo 01886
- 33. Dominici M, Le Blanc K, Mueller I, et al. Minimal criteria for defining multipotent

mesenchymal stromal cells. The International Society for Cellular position Therapy statement. Cytotherapy. 2006; 8(4):315-7. https://doi.org/10.1080/146532406008 55905

- 34. Gong W, Han Z, Zhao H, et al. Banking umbilical cord-derived human mesenchymal stromal cells for clinical use. Cell Transplant. 2012; 21(1):207-16. https://doi.org/10.3727/096368911X58 6756
- 35. Hernandez SL, Gong JH, Chen L, et al. Characterization of circulating and endothelial progenitor cells in patients with extreme-duration type 1 diabetes. Diabetes Care. 2014 Aug; 37(8):2193-201. https://doi.org/10.2337/dc13-2547
- 36. Hu CH, Tseng YW, Chiou CY, et al. Bone marrow concentrate-induced mesenchymal stem cell conditioned medium facilitates wound healing and prevents hypertrophic scar formation in a rabbit ear model. Stem Cell Res Ther. 2019 Aug 28; 10(1):275. https://doi.org/10.1186/s13287-019-1383-x
- 37. Burdick JA, Mauck RL, Gerecht S. To Serve and Protect: Hydrogels to Improve Stem Cell-Based Therapies. Cell Stem Cell. 2016 Jan 7; 18(1):13-5. https://doi.org/10.1016/j.stem.2015.12.
- 38. Levengood SL, Erickson AE, Chang FC, Zhang M. Chitosan-Poly(caprolactone) Nanofibers for Skin Repair. J Mater Chem B. 2017 Mar 7; 5(9):1822-1833. https://doi.org/10.1039/C6TB03223K
- 39. Ma K, Liao S, He L, Lu J, Ramakrishna S, Chan CK. Effects of nanofiber/stem cell composite on wound healing in acute full-thickness skin wounds. Tissue Eng Part A. 2011 May; 17(9-10):1413-24. https://doi.org/10.1089/ten.TEA.2010. 0373

Funding: The albino rats and devices were provided by the National Centre for Radiation Research and Technology (NCRRT).

Conflicts of interest: The authors declared no conflicts of interest related to this work.

Acknowledgements: The authors would like to thank Dr. Hassan Abd El-Reheem for providing the nanoscaffolds and Mohamed Farouk for his generous help during animal anesthesia and sacrifice.

Corresponding author:

Dr. Marwa M. Hegab Assistant Professor, Department of Oral Medicine and Periodontology Faculty of Oral and Dental Medicine Cairo University Cairo, Egypt

E-mail: marwa.hegab@dentistry.cu.edu.eg

Phone: +20 100 2084450

This is an open access article distributed under the Creative Commons Attribution-Noncommercial-NoDerivatives International (CC BY-NC-ND 4.0) License.